Mathematical Model for Aerodynamic Interaction of High-Speed Passenger and Freight Trains on Adjacent Tracks. Part II: Theoretical and Practical Basis for Solving the Problem in Complex Conditions

Marufdjan Rasulov[1,2], Masud Masharipov[1,2], Ramazon Bozorov[1,2] and Lazokat Kodirova[1,2]
[1]*Tashkent State Transport University, Temiryolchilar Str. 1, 100167 Tashkent, Uzbekistan*
[2]*University of Diyala, 32009 Baqubah, Diyala, Iraq*
tashiit_rektorat@mail.ru, masudcha@mail.ru, ramazon-bozorov@mail.ru, lazokaticegirl@gmail.com

Keywords: High-Speed, Aerodynamics, Safe Crossing, Curvature of Railway, Stability Coefficient, Empty Wagon, Freight Train, Standard, Air Current.

Abstract: The article studies the issues of mutual aerodynamic influence that affects the organization of safe crossing of high-speed passenger and freight trains when they move along adjacent railway tracks in difficult conditions (on curved sections of railways, under the influence of a strong side wind). At the same time, special attention is paid to the stability of the rolling stock. The reserve of the rollover stability coefficient for each unit of rolling stock was calculated depending on the radius of the curve of the railway section and the pressure of the side wind, and the limits of train speeds were set for their safe crossing in difficult conditions. The article also defines the limits of the safe crossing speeds of high-speed passenger and freight trains of different categories under these complex conditions under the curved conditions of the railways and the "Wind rose" study, which in turn is achieved to ensure the safety of train traffic. As a result, the effective use of train permeability and carrying capacity of railway sections is achieved.

1 INTRODUCTION

This scientific article serves as a logical continuation of the previous scientific study entitled "Mathematical model for aerodynamic interaction of high-speed passenger and freight trains on adjacent tracks, Part I: Preliminary conclusions on problem formulation and solution approach". The previous study focused on analyzing wind speeds using a 'wind rose' method and specifically examined double-track sections with mixed traffic and various types of trains operated by Uzbekistan Railways JSC, taking into account their geographical locations. By analyzing the areas where strong wind pressure may occur, an estimation was made regarding the margin of the stability coefficient for rolling stock units to prevent transverse overturning when trains traverse curved railway sections.

2 MATERIALS AND METHODS

When freight and high-speed passenger trains cross curved sections of the railway, the stability of the car is negatively affected due to the combination of centrifugal force and aerodynamic pressure forces caused by the resonance phenomenon. Figure 1 illustrates the forces acting on a unit of rolling stock moving along track 1. Considering that a high-speed passenger train experiences a greater force when moving along the same track compared to track 2, the maximum impact forces can be expressed as follows [1]-[3], [5]-[12].

$$\begin{cases} F_1^{total} = F_{y1} + F_2^{\text{centrifugal force}} \\ F_2^{total} = F_{y2} + F_1^{\text{centrifugal force}} \end{cases}. \quad (1)$$

Considering the reduction in the influence of aerodynamic force on movement along the 1st track, an increase in impact on movement along the 2nd track was observed. In this case, the calculation considered the centrifugal force, which is directly proportional to the square of the velocity and inversely proportional to the radius of curvature (refer to Figure 2).

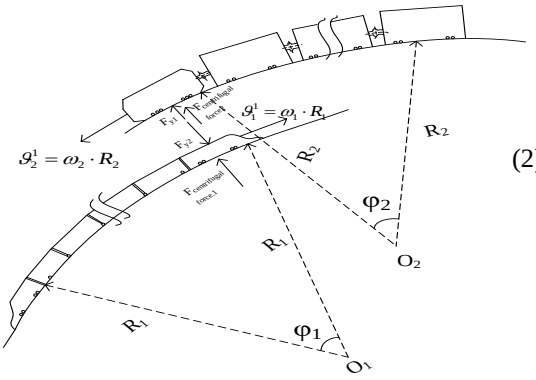

(2)

Figure 1: Influence of forces on a rolling stock unit on a railway track curve.

Furthermore, the calculations used standard values for undamped accelerations resulting from train movement on railway curves, which were determined for each traffic structure [4]-[6], [16]-[19].

$$F_2^{\text{centrifugal force}} = M_2 \cdot a_y^{freight}$$

$$F_1^{\text{centrifugal force}} = M_1 \cdot a_y^{high-speed}$$

$$a_y^{freight} = \frac{(\vartheta_2^1)^2}{3,6^2 \cdot R_{1,2}} \cdot cos(\gamma) - g \cdot sin(\gamma)$$

$$a_y^{high-speed} = \frac{(\vartheta_1^1)^2}{3,6^2 \cdot R_{1,2}} \cdot cos(\gamma) - g \cdot sin(\gamma) - g \cdot \alpha$$

Based on Figure 2 and considering that $tg(\gamma) \approx \sin(\gamma) \approx \frac{h}{2l}$ and $\cos(\gamma) \approx 1$ for small angles γ, (1) and (2) can be simplified to the following form:

$$\begin{cases} F_1^{total} \approx F_{y1} + M_2 \cdot \left(\frac{(\vartheta_2^1)^2}{3,6^2 \cdot R_{1,2}} - g \cdot \frac{h}{2l} \right) \\ F_2^{total} \approx F_{y2} + M_1 \cdot \left(\frac{(\vartheta_1^1)^2}{3,6^2 \cdot R_{1,2}} - g \cdot \frac{h}{2l} - g \cdot \alpha \right) \end{cases} \quad (3)$$

Here:

- S_1, S_2 - side surfaces of sections of high-speed passenger and freight trains, respectively, m^2.
- M_1, M_2 - Masses of high-speed passenger and freight trains, respectively, kg.
- α - inclination angle of the body of a high-speed train ($\alpha = 3° \approx 0{,}0523\, radian$).
- R_1, R_2 - radii of curvature respectively ($R_{1,2} \geq 1200\ m$), m.
- $\vartheta_1^1, \vartheta_2^1$ - maximum speeds of high-speed passenger and freight trains on curves, respectively ($160 \leq \vartheta_1^1 \geq 250\ km/h$, $25 \leq \vartheta_1^1 \geq 110\ km/h$), km/hour.
- h - height of the outer rail relative to the inner rail at railway bends ($h \leq 0{,}150\ м$), m.
- $2l$ - the width of the distance between the rims in the wheelset ($2l \cong 1{,}6\ m$), м.
- a_y - undamped lateral accelerations in curves ($-0{,}3 \leq a_y^{freight} \leq +0{,}3\ m/s^2$, $-0{,}7 \leq a_y^{\text{passenger train.}} \leq +0{,}7\ m/s^2$, $-1{,}2 \leq a_y^{\text{high-speed.}} \leq +1{,}2\ m/s^2$), m/s^2;
- g - acceleration of gravity ($g \approx 9{,}81\, m/s^2$), m/s^2.

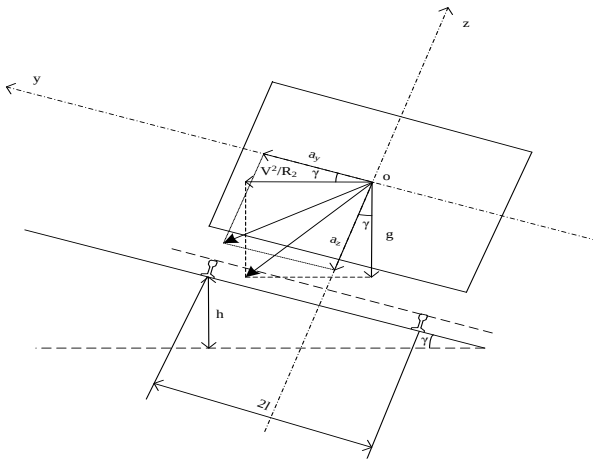

Figure 2: Components of centrifugal force and acceleration at railway turns.

In order to assess the mutual aerodynamic influence when combining high-speed passenger and freight trains on curved sections of the railway, it is crucial to consider the most challenging scenarios. The calculations were conducted using data obtained from sections capable of accommodating high-speed traffic within the Tashkent Railway Distance (PC-2) of UTY JSC [11]. Detailed results of these calculations are presented in Figures 3 and 4.

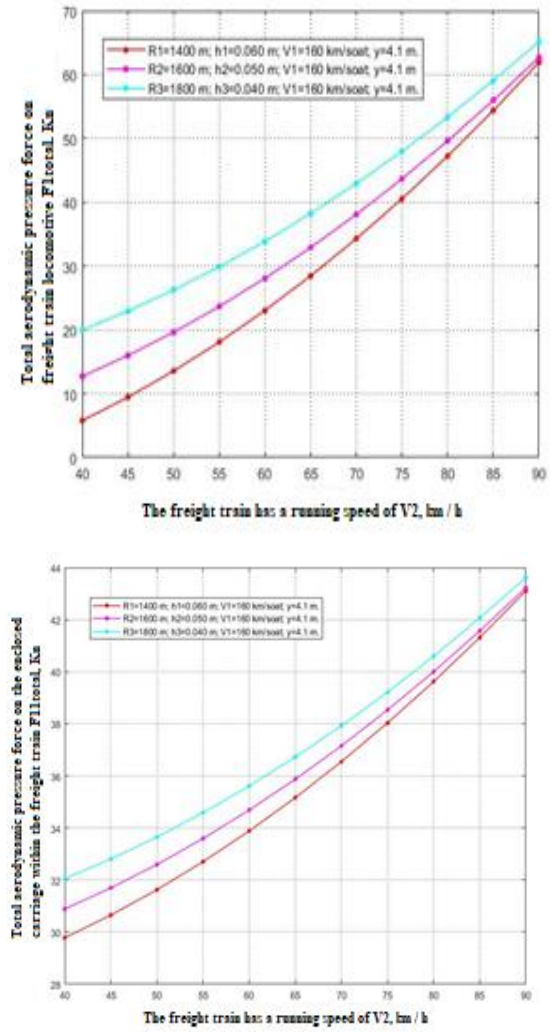

Figure 3: Sum of total aerodynamic forces on a freight train locomotive (left) and an empty four-axle universal closed car (right).

It is necessary to evaluate the margin of the stability coefficient to prevent transverse overturning caused by the total aerodynamic force acting on the components of the motion structure. To do this, the stability coefficient margin of an empty covered wagon, which represents a unit of rolling stock, is calculated in the transverse direction. The minimum acceptable values for the stability coefficient margin to prevent rollover in the transverse direction are determined as $K_{\text{stab.}}^{passenger} \geq 1{,}4$; $K_{\text{stab.}}^{empty\ car} \geq 1{,}3$; $K_{\text{stab.}}^{high-speed} \geq 1{,}6$ as stated in [12-15]. In the general case, the stability coefficient margin is determined by the following expression:

$$K_{\text{stab.}} = F_{st} \Big/ F_{dy} = F_{st} \Big/ (F_{\text{centrifugal force}} + F_{wind}^{aerody.}), \quad (4)$$

here, F_{st} , F_{dy} - static and dynamic forces from the wheel to the rail, kN, respectively.

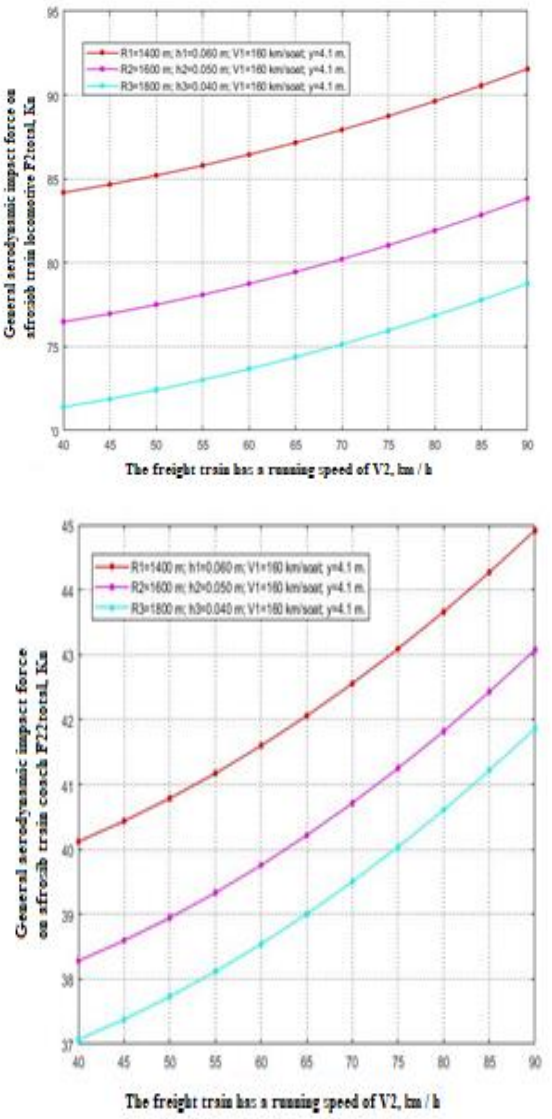

Figure 4: Sum of total aerodynamic forces on the locomotive (left) and cars (right) of a high-speed passenger train.

Based on reference, the dynamic force was determined using the following expression:

$$F_{dy} = F_k^{\text{centrifugal force}} \cdot \frac{h_k}{2l} + F_{w.k.}^{aerody.} \cdot \frac{h_{w.k}}{2l} + (F_t^{\text{centrifugal force.}} + F_{w.t.}^{aerody.}) \cdot \frac{r}{l} + F_k \cdot \frac{\Delta}{2l}. \quad (5)$$

The technical description of the universal four-axle boxcar is given in Table 1.

Table 1: Technical description of the universal four-axle boxcar.

Indicators	Amount
The weight of an empty wagon, KN	215,82
Weight capacity of a fully loaded wagon, KN	882,9
The distance from the level of the rail head to the center of gravity of the car body, m	3
The cross-sectional area of the side surface of the wagon, m^2	50,2
The length of the wagon between the truck axles, m (meters).	14,73
distance from the surface of the rail head to the geometric center of the side surface of the wagon body, m	2,87

The height of the resultant element of aerodynamic and centrifugal forces, considering the effect of wind in the transverse direction from the level of the rail head, was determined for empty wagons using expression (6):

$$h = \frac{F_{\text{centrifugal force.}} \cdot h_k + F_w^{aerody.} \cdot h_{w.k.}}{F_{\text{centrifugal force.}} + F_w^{aerody.}}. \quad (6)$$

Here, $F_{\text{centrifugal force.}}$, $F_w^{aerody.}$ - The aerodynamic forces, considering the effects of centrifugal force and wind, acting on the wagon body in the transverse direction, are measured in kilonewtons (kN).

h_k, h_{wk} - height of the point of application of aerodynamic forces, taking into account the influence of wind in the centrifugal and transverse directions from the level of the rail head, m.

The ratio of the forces acting on the car body in the transverse direction to the weight of the car body is determined by the following expression:

$$\gamma = \frac{F_{\text{centrifugal force}} + F_w^{aerody.}}{F_k}. \quad (7)$$

The displacement distance of the center of mass of empty cars in the transverse direction, under the influence of transverse forces, is determined by the following expression:

$$\begin{cases} \Delta = \frac{\gamma \cdot h_k}{(\frac{b_2^2}{f \cdot h} - 1)} \\ f = \frac{F_{tar} - 2 \cdot F_{bog} + 2 \cdot F_{part}}{4 \cdot c} \end{cases}. \quad (8)$$

The ratio of the mass of the bogie to the mass of its body is expressed by the following coefficient:

$$\delta = \frac{2 \cdot F_{bog}}{F_k}. \quad (9)$$

Based on the available data from reference [25], and considering expressions (5)-(9), expression (4) can be simplified as follows:

$$K_{stab.} = \frac{l \cdot (1+\delta)}{\gamma \cdot (h + r \cdot (1+\delta)) + \Delta}. \quad (10)$$

3 RESULT AND DISCUSSION

The calculations are based on the technical parameters of a two-axle truck 18-100. According to reference [13]-[14], considering the speed restrictions for high-speed passenger trains with radius of curvature values $R < 1200$ m (V1<160 km/h), a radius of curvature of $R = 1200$ m, and an outer rail lifting height of $h = 0{,}065$ m, the speed of trains was calculated. The calculations were performed based on the standard value of the stability factor for transverse overturning at m - the limit of safe crossing. Figures 5 and 6 present the "wind rose" and wind speed data for the respective regions during 2022, considering the geographical locations of the possible intersections.

To ensure the reliability of the results, it is crucial to consider challenging situations. For instance, in 2019, the highest wind speed was recorded in the desert regions of Bukhara-Navoi-Samarkand, reaching up to 30 m/s (108 km/h), with an external wind pressure of 500 Pa [20]-[21]. Similarly, in May 2022, the wind speed observed at Tashkent South Airport was 24 m/s (86 km/h), accompanied by an external wind pressure of 350 Pa. In the remaining months of the year, the average wind speed ranges from 40 to 45 km/h, with an external wind pressure of 100 Pa [19]. Taking these factors into account is essential for ensuring accurate and reliable calculations.

Based on the applied mathematical model, the dynamics of the overturning stability coefficient under the influence of different external wind loads was calculated. The calculations were performed using batch programming languages, and the results are presented in Tables 2-4. In these tables, the speed limits of the moving components are highlighted in green if stability is ensured and in red if stability is not ensured. Additionally, a detailed view of the developed program on the computer desktop can be seen in Figures 7-8.

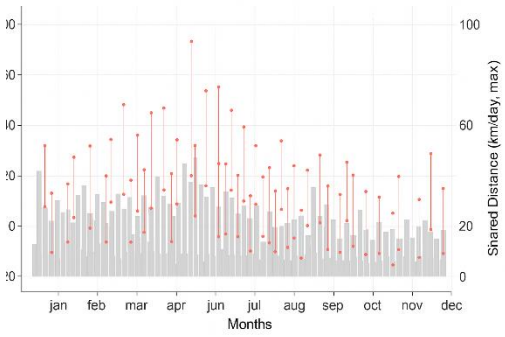

Tashkent South Airport

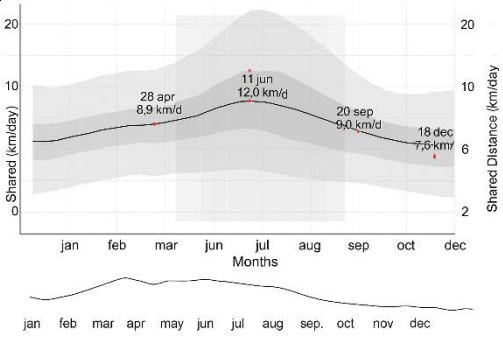

Yangiyol district

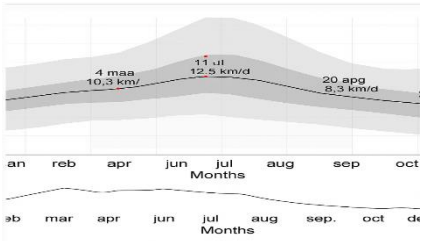

Chinaz district

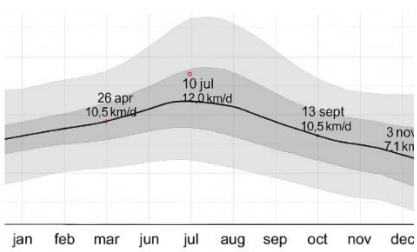

Gulistan district

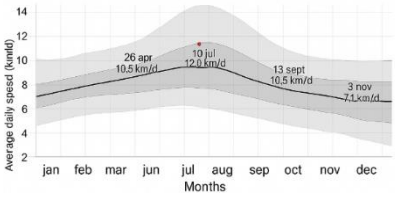

Yangiyer district

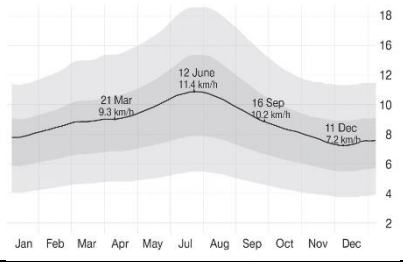

Jizzakh region

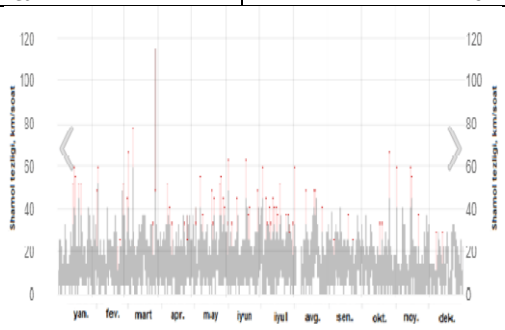

Samarkand region

Figure 5: Wind speed by region in 2022.

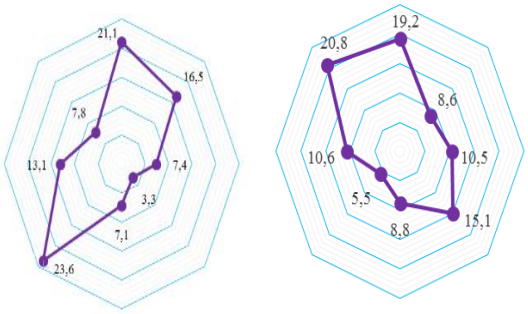

x

Figure 6: Wind rose patterns by regions in 2022.

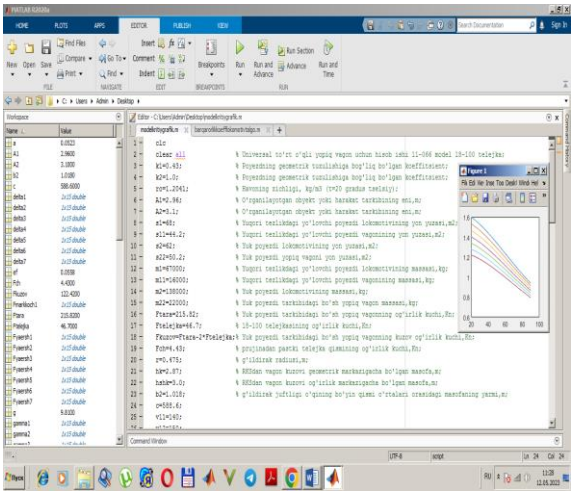

Figure 7: Visualization of the program displaying the dynamics of changes in the stability coefficient under the influence of various external wind pressures on the computer desktop.

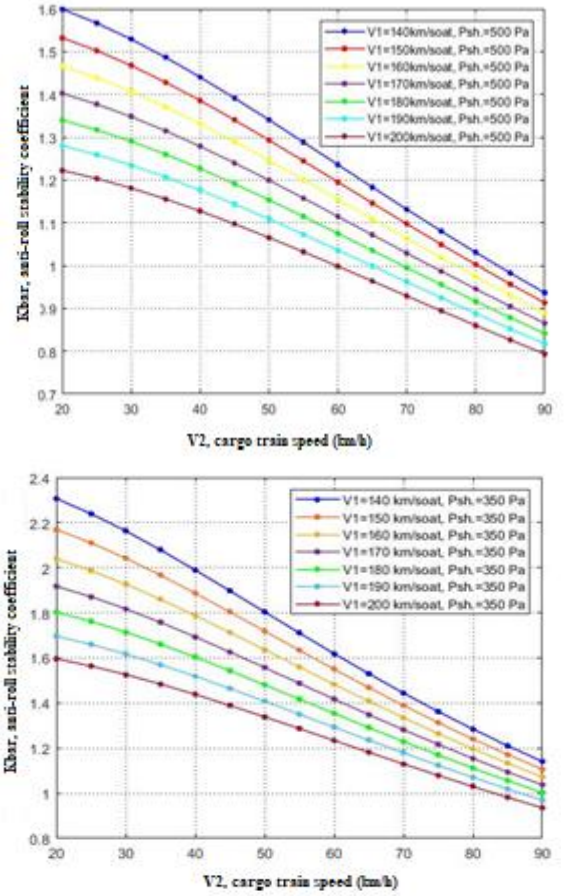

Figure 8: Calculation of the dynamics of changes in the stability coefficient under the influence of various external wind pressures.

Table 2: The limit of safe speeds for the crossing of trains is determined based on the standard value of the margin of the coefficient of stability against capsizing in the transverse direction ($P_{external\ wind.}$=500 Pa).

Speed of high-speed passenger train (V1), km/h	Freight train speed (V2), km/h	Aerodynamic pressure ($P_{aerody.}$), Pa	Reserve of the anti-rollover stability coefficient, $K_{stab.}^{empty\ car}$ (norm>1,3)	Reserve of the anti-rollover stability coefficient, $K_{stab.}^{high-speed}$ (norm >1,6)
External wind pressure $P_{external\ wind.}$ = 500 Pa				
140	25	155,3	1,567	1,830
	30	159,9	1,529	1,822
	35	165,3	1,487	1,812
	40	171,5	1,440	1,801
	45	178,6	1,391	1,788
	50	186,6	1,341	1,775
	55	195,3	1,288	1,760
	60	204,9	1,236	1,743
	65	215,3	1,183	1,726
	70	226,6	1,131	1,708
	75	238,7	1,080	1,689
	80	251,6	1,031	1,669
	85	265,4	0,983	1,648
	90	280,0	0,937	1,627

Table 3: The limit of safe speeds for the crossing of trains is determined based on the standard value of the margin of the coefficient of stability against capsizing in the transverse direction ($P_{external\ wind.}$=350 Pa).

Speed of high-speed passenger train (V1), km/h	Freight train speed (V2), km/h	Aerodynamic pressure ($P_{aerody.}$), Pa	Reserve of the anti-rollover stability coefficient, $K_{stab.}^{empty\ car}$ (norm>1,3)	Reserve of the anti-rollover stability coefficient, $K_{stab.}^{high-speed}$ (norm >1,6)
External wind pressure $P_{external\ wind.}$ = 350 Pa				
140	25	155,3	2,240	2,195
	30	159,9	2,163	2,183
	35	165,3	2,079	2,169
	40	171,5	1,990	2,154
	45	178,6	1,898	2,136
	50	186,6	1,804	2,117
	55	195,3	1,711	2,096
	60	204,9	1,619	2,074
	65	215,3	1,530	2,050
	70	226,6	1,445	2,025
	75	238,7	1,362	1,999
	80	251,6	1,284	1,971
	85	265,4	1,211	1,943
	90	280,0	1,141	1,914
150	25	176,7	2,110	1,829
	30	181,3	2,042	1,821
	35	186,7	1,967	1,811
	40	193,0	1,887	1,801
	45	200,1	1,804	1,789
	50	208,0	1,719	1,776
	55	216,8	1,634	1,762
	60	226,3	1,551	1,746
	65	236,8	1,469	1,730
	70	248,0	1,390	1,713
	75	260,1	1,313	1,695
	80	273,0	1,241	1,675
	85	286,8	1,172	1,656

4 CONCLUSIONS

This scientific study focuses on modeling the conditions for the safe passage of freight and high-speed passenger trains, with a particular emphasis on ensuring the stability of rolling stock units during crossings on curved sections of the railway. A mathematical model is utilized to calculate the stability factor against rollover in the transverse direction for each unit of rolling stock, taking into account the speed of trains.

The calculations were conducted with consideration given to the process of crossing high-speed passenger and freight trains on double-track sections of JSC “Uzbekistan temir yullari” that have mixed traffic of various train types, particularly in challenging situations involving railway curvature and the influence of external wind pressure. Based on the geographical location of the Uzbekistan-Khavast section and the average wind speed (pressure) in areas with consistent wind currents of 40-45 km/h (100 Pa) (Fig. 5-6), the maximum crossing speeds were determined to be 170 km/h for high-speed passenger trains and 60 km/h or 160 km/h for freight trains, as indicated by past three-year safe operation data (Table 4). The calculations revealed that with an external wind pressure of 350 Pa and above, the negative impact on the stability of an empty boxcar freight train becomes more pronounced. Consequently, when the speed of a high-speed

Table 4: The limit of safe speeds for the crossing of trains is determined based on the standard value of the margin of the coefficient of stability against capsizing in the transverse direction ($P_{external\ wind.}$=500 Pa).

Speed of high-speed passenger train (V1), km/h	Freight train speed (V2), km/h	Aerodynamic pressure ($P_{aerody.}$), Pa	Reserve of the anti-rollover stability coefficient, $K_{stab.}^{empty\ car}$ (norm>1,3)	Reserve of the anti-rollover stability coefficient, $K_{stab.}^{high-speed}$ (norm >1,6)
External wind pressure $P_{external\ wind.}$ = 100 Pa				
140	25	155,3	>2,415	3,279
	30	159,9	>2,415	3,254
	35	165,3	>2,415	3,225
	40	171,5	>2,415	3,192
	45	178,6	>2,415	3,155
	50	186,6	>2,415	3,116
	55	195,3	>2,415	3,073
	60	204,9	>2,415	3,028
	65	215,3	>2,415	2,980
	70	226,6	>2,415	2,930
	75	238,7	2,415	2,878
	80	251,6	2,180	2,824
	85	265,4	1,976	2,769
	90	280,0	1,797	2,714
150	25	176,7	>2,501	2,522
	30	181,3	>2,501	2,508
	35	186,7	>2,501	2,491
	40	193,0	>2,501	2,472
	45	200,1	>2,501	2,451
	50	208,0	>2,501	2,428
	55	216,8	>2,501	2,403
	60	226,3	>2,501	2,376
	65	236,8	>2,501	2,347
	70	248,0	2,501	2,317
	75	260,1	2,265	2,285
	80	273,0	2,057	2,252
	85	286,8	1,874	2,218
	90	301,4	1,712	2,184
160	25	199,6	>2,330	2,024
	30	204,2	>2,330	2,015
	35	209,6	>2,330	2,005
	40	215,9	>2,330	1,993
	45	223,0	>2,330	1,979
	50	230,9	>2,330	1,964
	55	239,7	>2,330	1,948
	60	249,3	>2,330	1,931
	65	259,7	>2,330	1,912
	70	270,9	2,330	1,892
	75	283,0	2,124	1,872
	80	296,0	1,940	1,850
	85	309,7	1,776	1,828
	90	324,3	1,630	1,804
	30	228,6	>2,172	1,667
	35	234,0	>2,172	1,660
	40	240,3	>2,172	1,652
	45	247,4	>2,172	1,643
	50	255,3	>2,172	1,632
	55	264,0	>2,172	1,621
	60	273,6	>2,172	1,610
	65	284,1	>2,172	1,597

passenger train is 150 km/h and the speed of a freight train exceeds 75 km/h, the stability coefficient against rollover of the train deviates from the standard value. However, within the specified crossing speeds (Table 3), trains can safely pass from the Tokimachi-Rakhimova station. In the Bukhara-Navoi-Samarkand regions, considering the strong wind (external wind pressure of 500 Pa) and railway curvature, the safe speed limit for crossing a high-speed passenger train was 140 km/h and for a freight train, it was 50 km/h. Train stability was ensured at these speeds (Table 2). Therefore, based on the developed mathematical model, it is possible to determine the possibilities of mutually safe crossings of high-speed passenger and freight trains on double-track sections with mixed traffic of various train types under any given conditions.

REFERENCES

[1] "EN 14067 Railway applications – Aerodynamics – Part 2: Aerodynamics on open track", ed: CEN/TC 256, 2010.

[2] "EN 14067 Railway applications – Aerodynamics – Part 4: Requirements and test procedures for aerodynamics on open track", ed: CEN/TC 256, 2010.

[3] Y. M. Lazarenko and A. N. Kapuskin, "Aerodynamic impact of the «Sapsan» high-speed electric train on passengers on platforms and on oncoming trains when crossing," Bulletin of the Research Institute of Railway Transport, no. 4, pp. 11-14, 2012.

[4] R. S. Raghunathan, H. D. Kim, and T. Setoguchi, "Aerodynamics of high-speed railway train," Progress in Aerospace Sciences, vol. 38, pp. 469-514, 2002.

[5] C. Baker, A. Quinn, M. Sima, L. Hoefener, and R. Licciardello, "Full-scale measurement and analysis of train slipstreams and wakes. Part 1: Ensemble averages," Proceedings of the Institute of Mechanical Engineers, Part F: Journal of Rail and Rapid Transit, pp. 453-467, 2013.

[6] C. Baker, A. Quinn, M. Sima, L. Hoefener, and R. Licciardello, "Full scale measurement and analysis of train slipstreams and wakes: Part 2 Gust analysis," Proceedings of the Institute of Mechanical Engineers, Part F: Journal of Rail and Rapid Transit, pp. 468-480, 2013.

[7] K. Matsumoto, K. Inoue, T. Hayashi, J. Okamoto, K. Hasegawa, and A. Hattori, "Effect of train draft on platforms and in station houses," JR East Technical Review, no. 16, pp. 39-42, 2010.

[8] H. Wu and Z. Zhou, "Study on aerodynamic characteristics and running safety of two high-speed trains passing each other under crosswinds based on computer simulation technologies," Journal of Vibroengineering, vol. 19, no. 8, pp. 6328-6345, 2017.

[9] T. Li, M. Li, Z. Wang, and J. Zhang, "Effect of the inter-car gap length on the aerodynamic characteristics of a high-speed train," Journal of Rail and Rapid Transit, no. 4, pp. 448-465, Sep. 2018.

[10] C. Baker, T. Johnson, D. Flynn, H. Hemida, A. Quinn, D. Soper, and M. Sterling, Train Aerodynamics fundamentals and applications, Butterworth-Heinemann, London, 2019, pp. 151-179, [Online]. Available: https://doi.org/10.1016/B978-0-12-813310-1.00008-3.

[11] "Instructions for determining the main parameters of the curves sections of the operated railways. P-28.01.2015y," no. 83-N.

[12] VSN-450-N, Departmental technical guidelines for design and construction. 1520 mm gauge railways, Tashkent: AO “UTY”, 2010.

[13] GOST 34093-2017, Vagoni passajirskie lokomotivnoy tyagi. Trebovaniya k prochnosti i dinamicheskim kachestvam, M.: Standartinform, 2017, 45 p.

[14] GOST 33211-2014, Vagoni gruzovie. Trebovaniya k prochnosti i dinamicheskim kachestvam, M.: Standartinform, 2016, 54 p.

[15] GOST 33788-2016, Vagoni gruzovie i passajirskie. Metodi ispitaniy na prochnost i dinamicheskie kachestva, M.: Standartinform, 2016, 41 p.

[16] M. Rasulov, M. Masharipov, S. Sattorov, and R. Bozorov, "Study of specific aspects of calculating the throughput of freight trains on two-track railway sections with mixed traffic," in E3S Web of Conferences, vol. 458, p. 03015, 2023, EDP Sciences, [Online]. Available: https://doi.org/10.1051/e3sconf/202345803015.

[17] M. Rasulov, M. Masharipov, S. E. Bekzhanova, and R. Bozorov, "Measures of effective use of the capacity of two-track sections of JSC “Uzbekistan Railways”," in E3S Web of Conferences, vol. 401, p. 05041, 2023, EDP Sciences, [Online]. Available: https://doi.org/10.1051/e3sconf/202340105041.

[18] A. Zbieć, "Aerodynamic Phenomena Caused by the Passage of a Train. Part 2: Pressure Influence on Passing Trains," Problemy Kolejnictwa, no. 192, pp. 195-202, Sep. 2021, [Online]. Available: http://dx.doi.org/10.36137/1926E.

[19] NB JT ST 03-98, Safety Standards for Railway Transport. Elektropoezda, M.: VNIIJT, 2003, 196 p.

[20] "Average Weather in Yangiyer, Uzbekistan Year-Round," [Online]. Available: https://weatherspark.com/y/106703/Average-Weather-in-Yangiyer-Uzbekistan-Year-Round.

[21] "Uzgidromet explained the causes of the hurricane on April 27," [Online]. Available: https://meteojurnal.ru/uzgidromet-obyasnil-prichiny-uragana-27-aprelya/.